MAGNETIC MODEL OF THE CERN PROTON SYNCHROTRON MAIN MAGNETIC UNIT

M. Juchno, EPFL, Lausanne, Switzerland, CERN, Geneva, Switzerland

Abstract

The CERN Proton Synchrotron (PS) will remain one of the key elements of the Large Hadron Collider (LHC) injector system for the next 20-25 years. Tuning the machine characteristics to the requirements for the LHC and its upgrades will require the establishment of an accurate magnetic model of the PS combined-function magnets, which is the subject of this paper. In the scope of this research, a detailed 2D quasi-static analysis of the PS magnets was performed, which allowed to investigate the magnetic field evolution and the contribution of separate magnet circuits at different field levels. An experimental validation of this new model was carried out through ad-hoc field measurements machine studies iterated with an optical model of the PS machine to recreate the measured optical parameters of the beam.

INTRODUCTION

During the next years, the PS will have to provide a reliable, high performance and highly versatile beam to meet the requirements of the LHC physics program and other experiments carried out at CERN. In order to perform further studies on improving the control over the beam optical parameters and reducing beam losses, it is essential to have precise knowledge of magnetic field and its harmonics in the main magnets. Therefore, it is important to develop a magnetic model that can be used as a fast and accurate source of magnetic field parameters needed in beam optics studies, in particular for adjusting the machine working point. The past approach to the creation of such model was limited only to the magnetic flux density and linear contribution of auxiliary circuits [1], but this model is not used at present. Derivation of the new nonlinear model formulas was based on a numerical calculation campaign and validation with field and beam-based measurements, since it is not possible to perform a dedicated measurement campaign within the whole spectrum of powering conditions needed to create a model of such a highly versatile machine as the PS.

Description of the PS Magnet

The PS main magnetic unit [2] is a normal conducting, combined-function magnet used to bend and vertically focus the particle beam. It is composed of two half-units: focusing and defocusing rigidly joined together, which introduce an alternating-gradient focusing. Each half-unit consists of 5 laminated, C-shaped iron blocks of either "open" or "closed" hyperbolic pole profile arranged in such a manner that a magnet has an arc shape with a bending radius r_0=70.0789 m and the overall length of 4260 mm along the orbit.

In the PS ring there are 100 magnets of four types that differ from each other by the placement of the iron back-leg with respect to the beam orbit and with the order of the focusing and the defocusing half-unit.

Coil System

The whole magnet is excited by two main coils wound around the top pole and the bottom pole piece. These coils are composed of two layers, each made of 5 aluminium conductor turns. There are two additional auxiliary coilstypes that are used to adjust the harmonics of the magnetic field: the figure-of-eight loop (F8) and the pole-face windings (PFW) (see Fig. 1). Due to different current direction in magnet halves, the figure-of-eight loop raises the field in one half and lowers in the other, and corrects the quadrupolar component of the field. The main purpose of the pole-face windings is the correction of the quadrupolar and the sextupolar component without significantly changing the dipole field. Each pole-face winding assembly is composed by two circuits called "wide" and "narrow", so that there are five auxiliary currents in total (I_{F8}, I_{FN}, I_{FW}, I_{DN} and I_{DW}) giving the possibility of controlling up to five optical parameters of the beam.
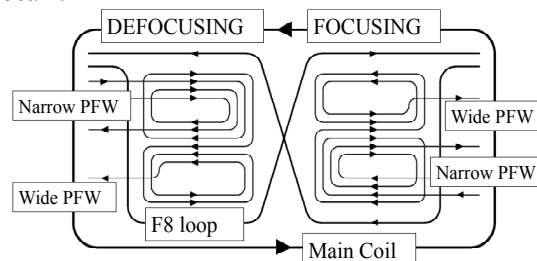

Figure 1: Sketch of the magnet windings.

NUMERICAL ANALYSIS

In order to obtain information of the magnetic field evolution under numerous powering conditions, a 2D quasi-static numerical analysis was performed using Opera 2D finite-element software package. The range of the main coil powering current was chosen to vary from 400 A to 5500 A. This corresponds to the range of the PS operations in which the beam is injected at a momentum of 2.12 GeV/c and it is accelerated and then extracted at 26 GeV/c. The magnetic field was computed for each variation of the powering currents summarised in Table 1, and the field coefficients up to sextupole were then derived with respect to the beam trajectory.

Table 1: Analysis Range

Circuit	Current range [A]	Current step [A]
Main coil	400,500-5500	250
Figure-of-eight loop	±1200	600
Pole-face windings	±200	100

MAGNETIC MODEL

Multipolar Decomposition

The multipolar components decomposed from the 2D numerical solution have been represented with Taylor series coefficients of the vertical field B_y expanded at the beam trajectory at $x_0 = 0$

$$K_n(x) = \left. \frac{d^{n-1} B_y(x)}{dx^{n-1}} \right|_{x=x_0},$$

which are expressed in $[T/m^{n-1}]$, in order to be directly comparable with experimental magnetic measurements performed with a Hall probe array. These coefficients have been obtained from an expansion with a discrete Fourier transform providing the field multipoles

$$B_n(r_0) = \frac{2}{N} \sum_{k=0}^{N-1} B_r(r_0, \varphi_k) \sin n\varphi_k,$$

where $\varphi_k = 2\pi k/N$ and $k=0,1,...,N-1$, and scaled to correspond to Taylor coefficients using the relation

$$K_n = \frac{(n-1)!}{r_0^{n-1}} B_n.$$

Main Circuit

An ideal hyperbolic pole made of a ferromagnetic medium with infinite permeability generates only the dipolar and the quadrupolar component of the magnetic field. However, due to limited pole width, finite permeability and effect of iron saturation, the pole of the PS magnet generates higher field components as well.

The vertical dipole component of the magnetic field can be obtained from a simplified magnetic circuit made of two elements connected in series: the magnetic core and the air gap, and written with a formula

$$B_y = NI \, T_f \, \eta_{mc}(NI)$$

where N is a number of conductor turns powered with current I, $T_f = \mu_0/g$ is a transfer function of the linear field and $\eta_{mc} = R_g/(R_g + R_c)$ is non-linear efficiency of the magnetic circuit. The efficiency of the main circuit is defined with reluctances of the circuit elements: iron core reluctance $R_c = l/A_c \mu_r \mu_0$ and gap reluctance $R_g = g/A_g \mu_0$, where l and g are the mean flux length in the iron core and the air gap, and A_c, A_g are effective flux cross-sections in the core and in the gap respectively. The field components defined in the sense of Taylor series expansion have a general form

$$K_{n,mc} = N_{mc} I_{mc} \, T_f \, H_{n,mc}(N_{mc} I_{mc}),$$

where

$$H_{n,mc} = \eta_n - (n-1) \frac{g'}{g} \eta_{n-1}$$

is the efficiency function of corresponding multipoles defined with derivatives of the main circuit efficiency

$$\eta_n(x) = \left. \frac{d^{n-1} \eta_{mc}(x)}{dx^{n-1}} \right|_{x=x_0}.$$

Auxiliary Coils

Total values of the magnetic field components obtained with the numerical analysis were decomposed into a sum of contributions of the main and all auxiliary magnet circuits $K_{n,tot} = K_{n,mc} + \Sigma_{aux} K_{n,aux}$. The magnetic field components generated by auxiliary coils were defined in a similar way as the components of the main circuit

$$K_{n,aux} = N_{aux} I_{aux} \, T_f \, H_{n,aux}(F_{n,aux}),$$

where $F_{n,aux} = N_{mc} I_{mc} + \Sigma_{aux} f_{n,aux} N_{aux} I_{aux}$ is an equivalent magnetomotive force that contains weighted contributions of each auxiliary circuit and affects auxiliary coils efficiencies.

Sigmoid Model of Efficiency Function

The efficiency function of each multipolar contribution depends on the spatial distribution of the magnetization over the cross-section of the magnet and on geometrical parameters (for example the mean flux length) which depend on the field level. As all these contributions are inter-linked, the efficiency function was modelled with a sum of normalizable sigmoid functions, such as hyperbolic tangent, which can accurately fit effects describing saturation contribution. Efficiency functions of the main circuit as well as each of the auxiliary coils can be expressed with a general formula

$$H_n(NI) = H_{n0} \left[1 + \sum_i \frac{\sigma_{ni}}{2} \left(1 + \tanh s_{ni} \frac{NI - NI_{sni}}{NI_{nom}} \right) \right],$$
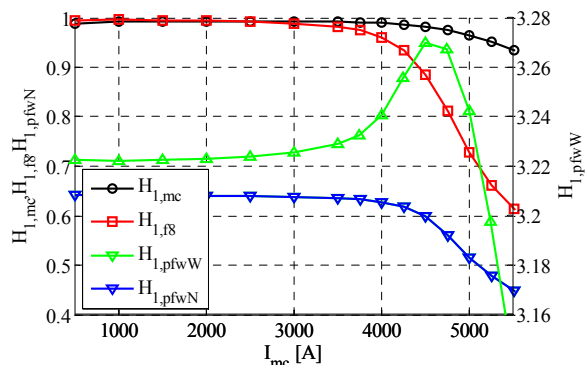

Figure 2: Dipole components of the main and auxiliary circuits efficiency function.

where H_{n0} is a linear component of the efficiency function and the σ_{ni}, s_{ni} and I_{ni} are the fitting parameters describing saturation (omitting the circuit index). An example of the efficiency functions behaviour at different main coil currents is shown in Fig. 2.

The complete quasi-static model of each of the field harmonics is described by two efficiency functions for the main focusing and the defocusing circuit, and a set of three efficiency functions for auxiliary coils, which apply to both magnet halves with a proper sign convention. Two-termed sigmoid model of the efficiency function gives sufficient accuracy. Thus, along with weights for the auxiliary currents, the magnetic model is described with 38 parameters for each of the field multipoles. Accuracy of the model compared to the numerical data is presented in Table 2.

Table 2: Accuracy Compared to Numerical Results

Multipole	K_1 [T]	K_2 [T/m]	K_3 [T/m^2]
δK_n	0.0004	0.0031	0.035

TUNE TRANSFER MATRICES

Field components calculated with the magnetic model were used as an input data for the optical MAD-X model of the machine [3] (see Fig. 3) to calculate the tune change due to variation of auxiliary currents and to recreate transfer matrices between powering currents and tune variations.

Defocusing half-unit (SBEND)   Focusing half-unit (SBEND)

Drift space (DRIFT)   Drift space (DRIFT)

Defocusing higher order components (MULTIPOLE)   Junction (SBEND)   Defocusing higher order components (MULTIPOLE)
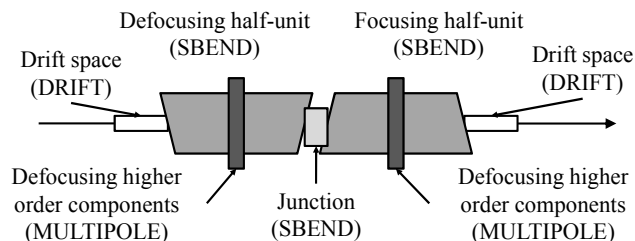
Figure 3: MAD-X model of the magnet.

Some of the model parameters, such as pole-face angles and effective bending length were approximated according to past experience. The quadrupolar and sextupolar coefficient in the junction between the magnet halves were fitted to match the initial tune and fixed to recreate relative tune variation. The comparison of measured [4] and calculated tune transfer matrices for two working points of 14 GeV/c and 26 GeV/c are presented in Table 3 and Table 4.

In case of the narrow focusing circuit elements, some discrepancies between the modelled values and measurements are visible, probably due to the beam radial

Table 3: Tune Transfer Matrix for 14 GeV/c

	ΔQ_h		ΔQ_v	
	Meas.	Calc.	Meas.	Calc.
ΔI_{F8}	-0.00121	-0.00128	0.00121	0.00130
ΔI_{PFN}	**0.00283**	**0.00502**	**-0.00128**	**-0.00321**
ΔI_{PFW}	0.00455	0.00473	-0.00322	-0.00244
ΔI_{PDN}	-0.00314	-0.00330	0.00512	0.00494
ΔI_{PDW}	-0.00268	-0.00257	0.00410	0.00461

Table 4: Tune Transfer Matrix for 26 GeV/c

	ΔQ_h		ΔQ_v	
	Meas.	Calc.	Meas.	Calc.
ΔI_{F8}	-0.00030	-0.00030	0.00030	0.00031
ΔI_{FN}	**0.00127**	**0.00263**	**-0.00063**	**-0.00177**
ΔI_{FW}	0.00253	0.00230	-0.00167	-0.00133
ΔI_{DN}	-0.00178	-0.00176	0.00280	0.00264
ΔI_{DW}	-0.00142	-0.00124	0.00214	0.00217

position at which the transfer matrices were measured. A further step will be to reoptimize the model taking into account a proper shift of the radial position and recreate the tune transfer matrix with better accuracy. It can be seen in Fig. 4 that for Δr of approximately 2.5 mm, the horizontal tune element of the matrix for the focusing narrow circuit should correspond to the vertical tune element for defocusing narrow circuit and vice versa, as it was computed with the model.
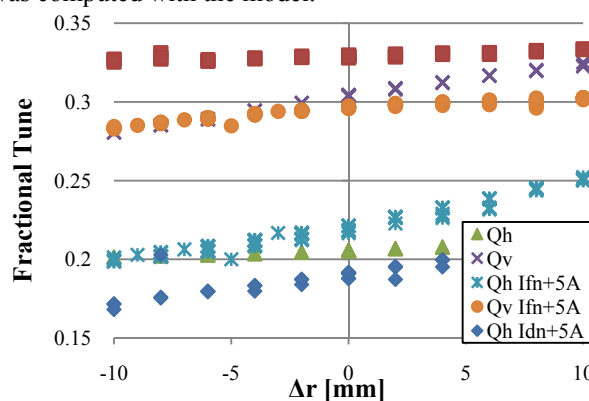
Figure 4: Measured tune variation at 14 GeV/c [4].

CONCLUSION AND OUTLOOK

The new magnetic model of the PS magnets implemented in a specifically adapted optical model of the PS accelerator was capable of reproducing measured transfer matrices between supply currents and machine tune variations.

A further increase of the magnetic model accuracy and most of all reproduction the chromaticity transfer functions will be provided by the results coming from 3D analysis, in particular for the magnetic effects between magnet halves.

REFERENCES

[1] T. Salvermoser, "Graphical Magnet Model", PS-PO Note 96-16, CERN, Geneva, 1996.

[2] K.H. Reich, "The CERN Proton Synchrotron Magnet", Technical Report MPS/Int. DL 63-13, CERN, Geneva, 1963.

[3] T. Risselada, "Beam Optics Data for the PS Ring and its Transfer Lines", PS-PA Note 92-04, CERN, Geneva, 1992.

[4] P. Freyermuth et al., "CERN Proton Synchrotron Working Point Matrix for Extended Pole Face Winding Powering Scheme", in Proceedings of IPAC 2010, (JACoW, Geneva, 2010) THPE019.